respectively. Unfortunately, however, a fraction of the target tumors are either refractory to corresponding tyrosine kinase inhibitors from the start of treatment or become resistant after an initial response.

In a case of EML4-ALK–positive non–small-cell lung cancer that became resistant to crizotinib after successful treatment for 5 months, we have discovered two de novo mutations in EML4-ALK, each of which confers resistance to the drug.

CASE REPORT

The patient was a 28-year-old man without a history of smoking who had received a diagnosis of lung adenocarcinoma, at a tumor–node–metastasis (TNM) clinical stage of T4N3M1, in April 2008. Given that the tumor did not harbor any EGFR mutations, the patient was treated with conventional chemotherapy. However, his tumor progressed after six cycles of three two-drug combinations. In November 2008, the presence of *EML4-ALK* variant 1 messenger RNA (mRNA)[1] in the tumor was confirmed by means of reverse transcription–polymerase-chain-reaction (PCR) analysis of a sputum sample. At this stage, the patient had large tumor nodules in the hilum of the right lung, multiple enlarged lymph nodes in the mediastinum, atelectasis in the right lung, and a massive effusion in the right pleural cavity (Fig. 1 in the Supplementary Appendix, available with the full text of this article at NEJM.org).

The patient was enrolled in the A8081001 study of crizotinib (ClinicalTrials.gov number, NCT00585195) on November 28, 2008, with oral administration of the drug at a dose of 250 mg twice per day. Within 1 week after the start of crizotinib treatment, his symptoms improved markedly. Although he had a partial response to the treatment, his pleural effusion was not completely eradicated (Fig. 1 in the Supplementary Appendix). After 5 months of treatment, however, the tumor abruptly started to grow again, resulting in a rapid expansion of the pleural effusion and in the development of tumors in both lungs (Fig. 1 in the Supplementary Appendix). The patient was withdrawn from the trial on May 25, 2009, and a sample of the pleural effusion in the right lung was then obtained for molecular analysis.

METHODS

DNA sequencing and characterization of the EML4-ALK mutants are described in detail in the Supplementary Appendix.

RESULTS

Because our patient's tumor resumed growth despite sustained administration of the ALK inhibitor crizotinib, we speculated that it might have acquired secondary genetic changes that confer resistance to the drug. Furthermore, given that resistance to tyrosine kinase inhibitors often results from acquired mutations within the target kinases,[7-9] we first examined the possibility that EML4-ALK itself had undergone amino acid changes.

Molecular analysis was performed on sputum specimens obtained before crizotinib treatment and pleural-effusion specimens obtained after relapse when treatment was stopped. Given that the proportion of tumor cells in the two types of specimens may have differed, we performed deep (high-coverage) sequencing of *EML4-ALK* complementary DNA (cDNA) derived from the specimens, using a high-throughput sequencer (Genome Analyzer II, Illumina) (Fig. 2 in the Supplementary Appendix). The sensitivity of our sequencing system, examined with the use of cDNA corresponding to the Janus kinase 3 (JAK3) amino acid mutation V674A[10] as a control, revealed that the maximum detection sensitivity was no more than one mismatched read per 6.50×10^5 total reads (Table 1 in the Supplementary Appendix).

Using deep sequencing, we detected a known single-nucleotide polymorphism, rs3795850, in the cDNA from the four specimens that were positive for *EML4-ALK* (Table 2 and Fig. 3 in the Supplementary Appendix). In addition, a T→C change at a position corresponding to nucleotide 4230 of human wild-type *ALK* cDNA (GenBank accession number, NM_004304) was detected at a low frequency (8.9%) in the sputum cDNA from our patient. Furthermore, two new alterations, G→A and C→A changes at positions corresponding to nucleotides 4374 and 4493 of wild-type *ALK* cDNA, were detected at frequencies of 41.8% and 14.0%, respectively, in the patient's pleural-effusion cDNA. There were no other recurrent alterations (present in 5% of reads) in the kinase-domain cDNA derived from any of the specimens.

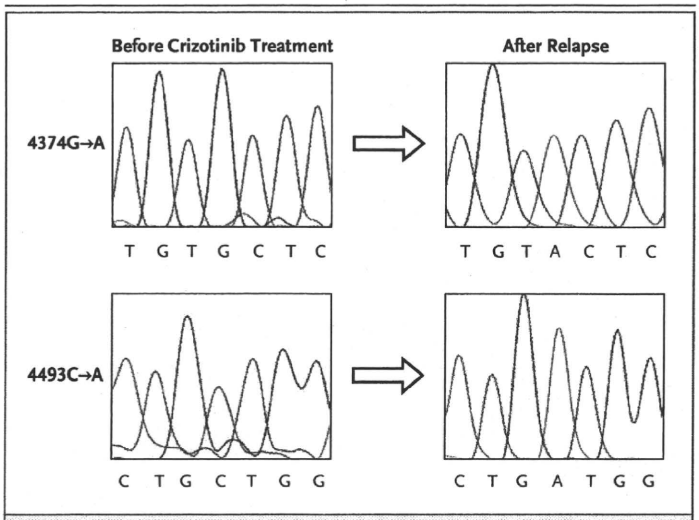

Figure 1. Secondary Mutations within *EML4-ALK*.

Electrophoretograms are shown for *EML4-ALK* cDNA clones prepared from sputum specimens obtained from our patient before crizotinib treatment and from pleural-effusion specimens obtained after relapse. The 4374G→A and 4493C→A mutations are present in the specimens obtained after relapse.

We next attempted to confirm these nucleotide changes by using Sanger sequencing. To rule out the possibility that the mutations had occurred in endogenous wild-type *ALK* rather than in *EML4-ALK*, we performed PCR with a forward primer targeted to *EML4* cDNA so that only the fusion cDNA would be amplified (Fig. 2 in the Supplementary Appendix). We did not detect the 4230T→C change among the 256 fusion cDNA clones derived from the patient's sputum specimens (data not shown), indicating that it was an artifact of the initial PCR or the deep-sequencing step. We did, however, readily confirm both 4374G→A and 4493C→A changes. Among 73 *EML4-ALK* cDNA clones from the patient's pleural-effusion specimens, 34 (46.6%) were positive for 4374G→A and 11 (15.1%) were positive for 4493C→A (Fig. 1). (The remaining 28 [38.4%] were negative for both point mutations.) These rates of detection are similar to those from the deep sequencing of *ALK*, indicating that wild-type *ALK* mRNA was present at a low level in lung tissue, as reported previously.[1]

The PCR analyses covered both nucleotide positions, yet none of the patient's specimens contained both mutations, indicating that each mutation occurred independently. Genomic fragments encompassing the 4374G and 4493C positions were also amplified by means of a PCR assay and were then subjected to nucleotide sequencing, which confirmed the presence of each of the two mutations in the tumor genome (Fig. 4 in the Supplementary Appendix).

The 4374G→A and 4493C→A substitutions result in cysteine→tyrosine (C→Y) and leucine→methionine (L→M) changes at the positions corresponding to amino acids 1156 and 1196, respectively, of wild-type human ALK (Fig. 2 in the Supplementary Appendix). We examined whether such amino acid changes affect the sensitivity of EML4-ALK to ALK inhibitors.

Cells of the mouse interleukin-3–dependent cell line BA/F3 that were made to individually express primary EML4-ALK and secondary mutant EML4-ALK (with the C1156Y or L1196M mutation) were exposed to ALK inhibitors. Crizotinib inhibited the growth of BA/F3 cells expressing primary EML4-ALK, in a concentration-dependent manner (Fig. 2A). In contrast, cells expressing either the C1156Y or L1196M mutant form manifested a markedly reduced sensitivity to the drug. Cells expressing the L1196M mutant form of EML4-ALK were more resistant to crizotinib than were those expressing the C1156Y mutant form (Fig. 2A, and Fig. 5 in the Supplementary Appendix).

We also examined whether cells expressing these EML4-ALK mutants are also refractory to other ALK inhibitors. A 2,4-pyrimidinediamine derivative (PDD) has a median inhibitory concentration for ALK of less than 10 nM,[11] and oral administration of PDD has been shown to eradicate lung-cancer nodules in transgenic mice with EML4-ALK expression.[4] BA/F3 cells expressing EML4-ALK with either the C1156Y or L1196M mutation were markedly less sensitive to PDD than were those expressing the primary EML4-ALK (Fig. 2A). Thus, although these mutations appear to develop during clinical treatment with crizotinib, their generation probably renders EML4-ALK resistant not only to crizotinib but also to other ALK inhibitors. In contrast to the resistance profile for crizotinib, BA/F3 cells expressing the EML4-ALK C1156Y mutant form were slightly more resistant to PDD than were those expressing the L1196M mutant form (Fig. 2A, and Fig. 6 in the Supplementary Appendix), indicating that the resistance profiles for the two mutations may be, in part, inhibitor-dependent, as was previously shown for BCR-ABL mutants.[12]

We examined tyrosine phosphorylation of

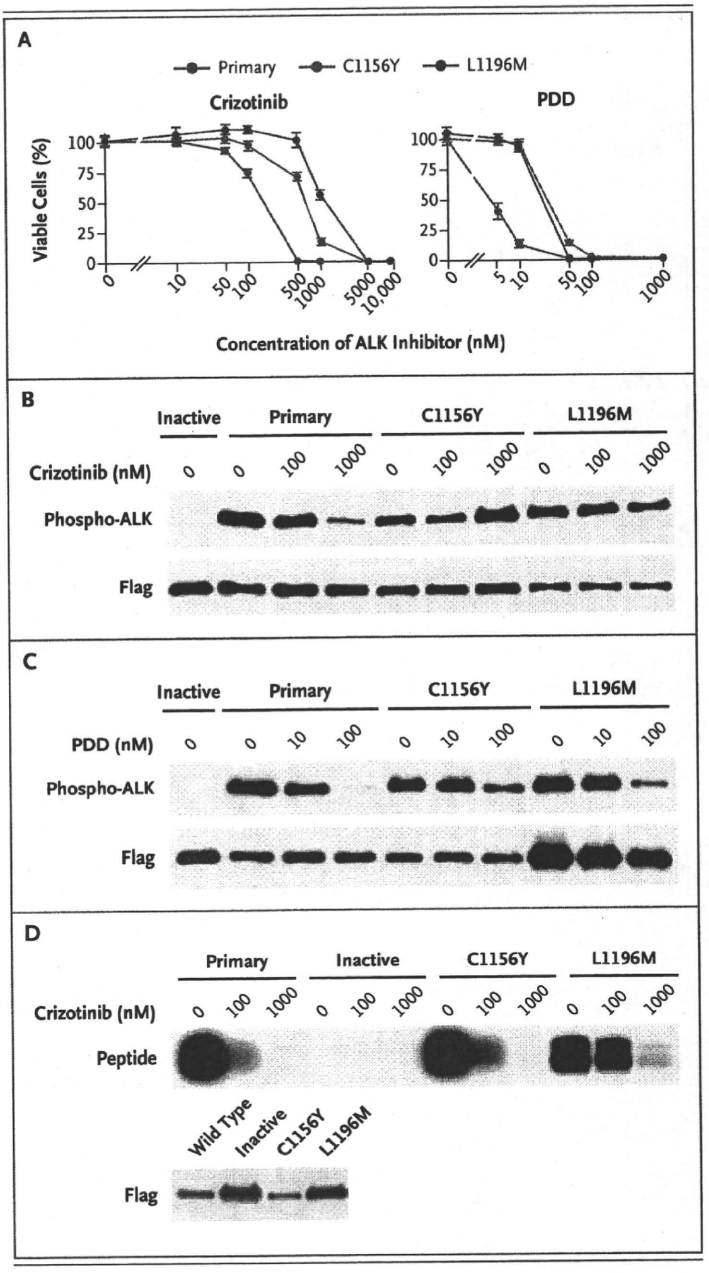

Figure 2. Properties of EML4-ALK with Secondary Mutations.

Panel A shows the percentage of viable BA/F3 cells expressing primary EML4-ALK, EML4-ALK with the C1156Y mutation, or EML4-ALK with the L1196M mutation, after 5×10^5 cells were incubated for 48 hours with the indicated concentration of crizotinib (left) or 2,4-pyrimidinediamine derivative (PDD) (right). Data are expressed as the mean value, from three separate experiments, for the percentage of cells expressing primary EML4-ALK after incubation in the vehicle (dimethyl sulfoxide) only. The I bars indicate standard deviations. Because primary EML4-ALK, EML4-ALK with the C1156Y mutation, and EML4-ALK with the L1196M mutation each abrogate the interleukin-3 dependence of BA/F3 cells, the assays were performed in the absence of the interleukin. Panels B and C show the effect of ALK inhibitors on EML4-ALK and its secondary mutant forms, tagged with the Flag epitope, in BA/F3 cells. Panel B shows the results of exposure to various concentrations of crizotinib for 15 hours, after which EML4-ALK was immunoprecipitated from cell lysates with antibodies against the Flag epitope and the immunoprecipitate was subjected to immunoblot analysis with the use of antibodies specific for ALK phosphorylated at the tyrosine at position 1604 (Phospho-ALK) or for the Flag epitope. Cells expressing an inactive mutant form of EML4-ALK were examined as a negative control. Panel C shows the results of a similar experiment, involving PDD instead of crizotinib. Panel D shows the results of an in vitro kinase assay for Flag-tagged EML4-ALK or its secondary mutants immunoprecipitated from BA/F3 cells with antibodies against the Flag epitope. The immunoprecipitates were incubated with [γ-^{32}P]ATP, a synthetic peptide, and various concentrations of crizotinib (top). Separate immunoprecipitate samples were subjected to immunoblot analysis with antibodies against the Flag epitope (bottom).

EML4-ALK by means of immunoblot analysis, using antibodies specific for ALK phosphorylated at the tyrosine at position 1604. The exposure of BA/F3 cells to crizotinib markedly inhibited the tyrosine phosphorylation of EML4-ALK but did not substantially affect that of the C1156Y and L1196M mutants (Fig. 2B). Exposure to PDD also inhibited the tyrosine phosphorylation of EML4-ALK, in a concentration-dependent manner, with a lesser effect on the mutants (Fig. 2C). The results of an in vitro kinase assay were consistent with these findings, showing pronounced inhibition of the enzymatic activity of primary EML4-ALK with crizotinib, whereas the effect on the C1156Y mutant was less pronounced and the effect on the L1196M mutant was much less pronounced (Fig. 2D).

Figure 3 shows the cysteine at position 1156 (C1156) and the leucine at position 1196 (L1196) of the kinase domain of ALK.[13] C1156 is positioned adjacent to the N-terminal of the predicted helix αC as well as close to the upper edge of the ATP-binding pocket. No activating mutations have been reported at this position in other tyrosine kinases in cancer specimens. L1196 of ALK corresponds to the threonine at position 315 in ABL and at position 790 in EGFR, each of which is the site of the most fre-

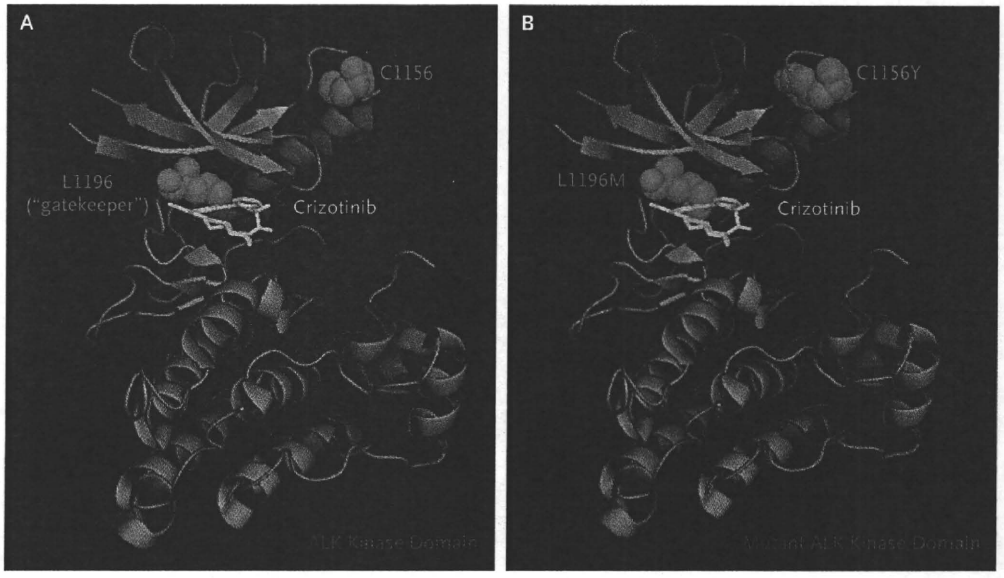

Figure 3. Predicted Crystal Structure of the Kinase Domain of ALK.
Panel A shows the nonmutant kinase domain and the site of binding of crizotinib. Panel B shows the EML4-ALK secondary mutations at positions 1156 and 1196. Adapted from Bossi and colleagues.[13]

quently acquired mutations that confer resistance to tyrosine kinase inhibitors in these kinases (Fig. 7 in the Supplementary Appendix).[14,15] This site is located at the bottom of the ATP-binding pocket (Fig. 3), and the presence of an amino acid with a bulky side chain at this "gatekeeper" position may interfere with the binding of many tyrosine kinase inhibitors.[7,16]

DISCUSSION

We identified two de novo mutations within the kinase domain of EML4-ALK from the tumor of a single patient that confer resistance to multiple ALK inhibitors. Given that we did not detect any *EML4-ALK* cDNA harboring both mutations, we propose that each mutation developed independently in distinct subclones of the tumor. Because we were not able to examine pleural-effusion specimens from the patient before he received crizotinib treatment, we do not know whether the resistant clones were present initially or developed secondarily, during the treatment.

Amino acid substitutions at the gatekeeper position of several tyrosine kinases have been detected in tumors treated with tyrosine kinase inhibitors (Fig. 7 in the Supplementary Appendix).[7-9,17,18] Whereas no mutations at this site have previously been reported for EML4-ALK or ALK, the effects of various artificial amino acid substitutions at the gatekeeper position of nucleophosmin (NPM)–ALK, another fusion-type "oncokinase" form of ALK, were recently examined.[19] The findings were consistent with the results of our analysis of tumor cells in vivo: the introduction of methionine at this position rendered NPM-ALK resistant to ALK inhibitors. It is therefore likely that gatekeeper alterations constitute a universal mechanism for the acquisition of tyrosine kinase–inhibitor resistance in oncogenic tyrosine kinases.

In contrast to gatekeeper substitutions, activating mutations at the position adjacent, on the N-terminal side, to the αC helix (e.g., C1156 in ALK) have not been confirmed for other tyrosine kinases in cancer specimens. Though a T→I change at the corresponding position of EGFR was described in one case of non–small-cell lung cancer, its relevance to drug sensitivity was not examined.[16] The importance of helix αC for allosteric regulation of enzymatic activity has been shown, however, for serine–threonine kinases.[20] A change at C1156 of ALK might therefore interfere allosterically with the binding of tyrosine

kinase inhibitors. Determination of the crystal structure of the ALK kinase domain with the C1156Y or L1196M mutation should shed light on these matters, as well as provide a basis for the development of next-generation ALK inhibitors that may effectively eradicate tumors harboring EML4-ALK with the acquired mutations.

Supported in part by grants from the Ministry of Health, Labor, and Welfare of Japan; the Ministry of Education, Culture, Sports, Science, and Technology of Japan; and the Japan Society for the Promotion of Science.

Disclosure forms provided by the authors are available with the full text of this article at NEJM.org.

We thank Y.-J. Bang and the medical staff at Seoul National University Hospital for their support in the treatment of this patient, as well as Y. Togashi and S. Hatano for technical assistance.

REFERENCES

1. Soda M, Choi YL, Enomoto M, et al. Identification of the transforming EML4-ALK fusion gene in non-small-cell lung cancer. Nature 2007;448:561-6.
2. Mano H. Non-solid oncogenes in solid tumors: EML4-ALK fusion genes in lung cancer. Cancer Sci 2008;99:2349-55.
3. Horn L, Pao W. EML4-ALK: honing in on a new target in non-small-cell lung cancer. J Clin Oncol 2009;27:4232-5.
4. Soda M, Takada S, Takeuchi K, et al. A mouse model for EML4-ALK-positive lung cancer. Proc Natl Acad Sci U S A 2008;105:19893-7.
5. Druker BJ, Talpaz M, Resta DJ, et al. Efficacy and safety of a specific inhibitor of the BCR-ABL tyrosine kinase in chronic myeloid leukemia. N Engl J Med 2001;344:1031-7.
6. Mok TS, Wu YL, Thongprasert S, et al. Gefitinib or carboplatin-paclitaxel in pulmonary adenocarcinoma. N Engl J Med 2009;361:947-57.
7. Shah NP, Nicoll JM, Nagar B, et al. Multiple BCR-ABL kinase domain mutations confer polyclonal resistance to the tyrosine kinase inhibitor imatinib (STI571) in chronic phase and blast crisis chronic myeloid leukemia. Cancer Cell 2002;2:117-25.
8. Kobayashi S, Boggon TJ, Dayaram T, et al. EGFR mutation and resistance of non–small-cell lung cancer to gefitinib. N Engl J Med 2005;352:786-92.
9. Pao W, Miller VA, Politi KA, et al. Acquired resistance of lung adenocarcinomas to gefitinib or erlotinib is associated with a second mutation in the EGFR kinase domain. PLoS Med 2005;2(3):e73.
10. Choi YL, Kaneda R, Wada T, et al. Identification of a constitutively active mutant of JAK3 by retroviral expression screening. Leuk Res 2007;31:203-9.
11. Choi YL, Takeuchi K, Soda M, et al. Identification of novel isoforms of the EML4-ALK transforming gene in non-small cell lung cancer. Cancer Res 2008;68:4971-6.
12. Branford S, Melo JV, Hughes TP. Selecting optimal second-line tyrosine kinase inhibitor therapy for chronic myeloid leukemia patients after imatinib failure: does the BCR-ABL mutation status really matter? Blood 2009;114:5426-35.
13. Bossi RT, Saccardo MB, Ardini E, et al. Crystal structures of anaplastic lymphoma kinase in complex with ATP competitive inhibitors. Biochemistry 2010;49:6813-25.
14. Deininger M, Buchdunger E, Druker BJ. The development of imatinib as a therapeutic agent for chronic myeloid leukemia. Blood 2005;105:2640-53.
15. Linardou H, Dahabreh IJ, Bafaloukos D, Kosmidis P, Murray S. Somatic EGFR mutations and efficacy of tyrosine kinase inhibitors in NSCLC. Nat Rev Clin Oncol 2009;6:352-66.
16. Carter TA, Wodicka LM, Shah NP, et al. Inhibition of drug-resistant mutants of ABL, KIT, and EGF receptor kinases. Proc Natl Acad Sci U S A 2005;102:11011-6.
17. Cools J, DeAngelo DJ, Gotlib J, et al. A tyrosine kinase created by fusion of the PDGFRA and FIP1L1 genes as a therapeutic target of imatinib in idiopathic hypereosinophilic syndrome. N Engl J Med 2003;348:1201-14.
18. Tamborini E, Bonadiman L, Greco A, et al. A new mutation in the KIT ATP pocket causes acquired resistance to imatinib in a gastrointestinal stromal tumor patient. Gastroenterology 2004;127:294-9.
19. Lu L, Ghose AK, Quail MR, et al. ALK mutants in the kinase domain exhibit altered kinase activity and differential sensitivity to small molecule ALK inhibitors. Biochemistry 2009;48:3600-9.
20. Hindie V, Stroba A, Zhang H, et al. Structure and allosteric effects of low-molecular-weight activators on the protein kinase PDK1. Nat Chem Biol 2009;5:758-64.

Acta Med. Okayama, 2010
Vol. 64, No. 5, pp. 285-291

Acta Medica Okayama
http://escholarship.lib.okayama-u.ac.jp/amo/

Original Article

Cancer of Unknown Primary Site: A Review of 28 Cases and the Efficacy of Cisplatin/Docetaxel Therapy at a Single Institute in Japan

Hisakazu Nishimori[a,b]*, Shunji Takahashi[a], Katsuyuki Kiura[b], Daisuke Ennishi[a,b], Takayuki Kobayashi[a], Koji Sano[a], Eiji Shinozaki[a], Masahiro Yokoyama[a], Yuko Mishima[a], Yasuhito Terui[a], Keisho Chin[a], Nobuyuki Mizunuma[a], Yoshinori Ito[a], Seiichiro Nishimura[c], Kengo Takeuchi[d], Yuichi Ishikawa[d], Masahiko Oguchi[e], Mitsune Tanimoto[b], and Kiyohiko Hatake[a]

[a]Division of Medical Oncology and Hematology, Cancer Institute Hospital, Koto-ku, Tokyo 135-8550, Japan,
[b]Department of Hematology, Oncology, Allergy, and Respiratory Medicine, Okayama University Hospital, Okayama 700-8558, Japan,
Divisions of [c]Breast Surgery, [e]Radiology, Cancer Institute Hospital, and
[d]Division of Pathology, Cancer Institute of the Japanese Foundation for Cancer Research, Koto-ku, Tokyo 135-8550, Japan

We evaluated the efficacy and toxicity of cisplatin/docetaxel (CDDP/TXT) chemotherapy and identified prognostic factors in Japanese patients with cancer of unknown primary site (CUP). Twenty-eight consecutive patients seen at a single institute were reviewed retrospectively. Sixteen patients were treated with TXT 80 mg/m², followed by CDDP 75 mg/m². The overall response rate to CDDP/TXT treatment was 62.5%, with a median survival time (MST) of 22.7 months. Common adverse reactions were myelosuppression and hyponatremia. The MST of all 28 patients with CUP was 8.3 months, and the 1-year overall survival rate was 45.6%. Univariate analysis identified 5 prognostic factors:performance status, liver involvement, bone involvement, pleural involvement, and lymph node involvement. In conclusion, CDDP/TXT chemotherapy is effective with tolerable toxicity in patients with CUP. Japanese patients with CUP might be chemosensitive and may survive longer.

Key words: cancer of unknown primary site (CUP), cisplatin, docetaxel, prognosis

Cancer of unknown primary site (CUP) is defined as the presence of metastatic cancer documented in the absence of an identifiable primary tumor site. These tumors are not rare; they represent 3-5% of all malignancies diagnosed in oncology practice [1, 2]. CUP occurs in a heterogeneous group of patients, and subgroups with treatment-responsive diseases exist that may achieve long-term, disease-free survival [1]. Generally, however, the prognosis of CUP is poor, with median survival times of 6-12 months, and the benefits of chemotherapy compared with best supportive care remain unclear [3].

Chemotherapy for patients with CUP is improving, but no chemotherapy regimen has been established as a standard first-line therapy for these patients [2]. Recent clinical reports have shown that cisplatin (CDDP)-containing regimens have good response rates of 32-55% in patients with CUP and are relatively well-tolerated [3, 4]. Docetaxel (TXT) has definite antitumor activity in various solid tumors and seems to

Received March 17, 2010; accepted May 21, 2010.
*Corresponding author. Phone:+81-86-235-7227; Fax:+81-86-232-8226
E-mail:n-mori@md.okayama-u.ac.jp (H. Nishimori)

be a good candidate for inclusion in a chemotherapy regimen for patients with CUP [5]. A CDDP plus TXT phase II study revealed a 26% response rate with 42% 1-year survival [6].

This paper presents a retrospective analysis of 28 consecutive Japanese patients with CUP to clarify the disease course and prognostic factors. We also report an excellent response rate and survival of Japanese patients with CUP who were treated using a combination regimen of CDDP/TXT.

Patients and Methods

Patients. Twenty-eight consecutive patients referred to the Division of Medical Oncology and Hematology at the Cancer Institute Hospital between April 1, 2000 and September 30, 2004 were reviewed retrospectively. Patients referred with a presumed diagnosis of CUP were identified and registered in the database at the time of their initial clinical evaluation. All patients diagnosed with CUP during this period were registered; however, 2 female patients with adenocarcinoma involving only the axillary lymph nodes were treated for occult breast cancer and were excluded from this analysis. The medical records of the patients were reviewed for the results of diagnostic studies and pathologic and cytologic diagnosis before referral, the results of subsequent radiographic evaluations, pathology review, involved disease sites, treatment, and survival.

Clinical evaluation. All patients with CUP underwent a basic evaluation consisting of a complete medical history, a physical examination (including careful palpation of the thyroid, breasts, lymph nodes, and prostate), general laboratory studies, chest radiography, and computed tomography from the neck to pelvis. If possible, gastrointestinal endoscopy, nose and pharyngeal endoscopy, and bronchoscopy were conducted. Positron emission tomography (PET) was performed in some patients when all other tests were inconclusive. In some cases, an extensive immunohistochemical study was carried out with the biopsied specimen to minimize the possibility of a misdiagnosis of other malignancies such as non-Hodgkin's lymphoma, extragonadal germ cell tumor, malignant melanoma, or undifferentiated sarcoma [2]. The most commonly used markers were the leukocyte common antigen, cytokeratins, neuron-specific enolase or chromogranin, S-100 protein, vimentin, thyroid transcription factor-1 (TTF-1), estrogen receptors, HMB45, and prostate-specific antigen (PSA). The blood concentrations of CA19-9, CA15-3, CA125, and carcinoembryonic antigen (CEA) were assessed in most cases.

Decision-making in the 'cancer board meeting'. Determining whether the primary site is unknown or whether it will be possible to detect with further evaluation is difficult. In the present study, members of the cancer board, including medical oncologists, hematologists, surgeons, pathologists, and radiation oncologists, evaluated the diagnosis and treatment strategies for the patients with CUP.

Treatment schedule for CDDP/TXT therapy. Eligible patients with CUP were treated with CDDP/TXT combination chemotherapy. All patients gave written informed consent. TXT 80 mg/m^2 in 300 mL of normal saline was administered over 2 h, followed by CDDP 75 mg/m^2, which was administered via a 120-min intravenous infusion. Premedication included intravenous administration of 4 mg of dexamethasone 24 h before treatment, 30 min before starting the docetaxel infusion, and 24 h after the infusion. A single 3-mg intravenous dose of granisetron was given to all patients as an antiemetic. Concurrent radiotherapy for symptom control in the absence of disease progression was allowed, but the drugs were held for at least 2 weeks after irradiation. Chemotherapy cycles were repeated every 3 weeks. Doses were modified for some patients mainly due to hematological toxicity.

Assessment of response and toxicity. Responses were defined according to the World Health Organization criteria [7]. Briefly, complete response (CR) was defined as the entire disappearance of all assessable lesions and signs of disease for at least 4 weeks. Partial response (PR) was defined as a reduction of 50% or more in the sum of the products of the perpendicular dimensions of measurable lesions and the appearance of no new lesion for at least 4 weeks. No change (NC) was defined as a decrease of less than 50% or an increase of less than 25% in the 2 greatest dimensions of measurable lesions and the appearance of no new lesions. Progressive disease (PD) was defined as any evidence of disease progression of 25% or more, or the appearance of a new lesion. Chemotherapy-related adverse events were recorded according to the National Cancer Institute's Common

Terminology Criteria, version 3.0 [8].

Statistical methods. Survival was calculated from the first day of pathologically or cytologically diagnosed malignancy. Survival following CDDP/TXT therapy was calculated from the first day of treatment. Survival curves were estimated using the Kaplan-Meier method [9] and compared using the Cox-Mantel log-rank test [10]. StatView 5.0 (SAS Institute, Cary, NC, USA) was used for the statistical analyses.

Results

General patient characteristics. The characteristics of our 28 patients (19 men and 9 women) are listed in Tables 1 and 2. One female patient was excluded from the survival analysis because she was postoperatively diagnosed with ovarian cancer. The median age at diagnosis was 58.5 years (range 32–76 years). Performance status according to the Eastern Cooperative Oncology Group (ECOG) [11] was 0–1 in 17 patients (60.7%). The sites of metastasis documented pathologically, cytologically, or radiographically are listed in Table 3. Lymph nodes were involved most frequently (64.3%), and visceral metastases including bone, lung, or liver were also common. The lymph node involvement was further subclassified by anatomic site. Of the 18 patients with nodal metastases, 11 had retroperitoneal, 8 had supraclavicular or cervical, 7 had mediastinal, 4 had axillary, and 4 had inguinal lymph nodes.

Table 1 Characteristics of 28 CUP patients

Characteristic	No. of Patients
Sex	
Female	9
Male	19
Age, years	
0–40	1
41–50	6
51–60	8
61–70	10
71–80	3
Median	58.5
Range	32–76
Performance status	
0–1	17
2–3	11

The pathological diagnoses of the patients are also listed in Table 2. Thirteen patients (46.4%) were diagnosed with adenocarcinoma, 9 (32.1%) with poorly differentiated carcinoma, 2 (7.1%) with squamous cell carcinoma, and 4 with unknown or other diagnoses. One patient was diagnosed based only on the cytology of ascites. No patients with neuroendocrine carcinoma were included in this study. No patients appeared to belong to subgroups with a favorable prognosis [1].

Twelve patients (42.9%) had a single metastatic organ site, 4 (14.3%) had 2, 7 (25.0%) had 3, and 5 (17.9%) had 4 or more. Serum tumor markers at baseline were assessed in all 16 patients who underwent CDDP/TXT therapy.

Twenty-five patients (89.3%) were treated with chemotherapy with or without concurrent radiotherapy for symptom control. One patient was treated with radiotherapy only. Two patients were treated with supportive care alone.

CDDP/TXT treatment. Sixteen patients who received the CDDP/TXT combination according to the protocol were assessable for response. The patient

Table 2 Sites of tumor involvement and histologic diagnoses in 28 patients with CUP

Site of involvement	No. of patients
Lymph nodes	18
Bone	10
Lung	7
Liver	6
Pleura/pleural space	4
Peritoneum	4
Skin	3
Adrenal	2
Others	9
Histologic Diagnosis	**No. of patients**
Adenocarcinoma	13
Poorly differentiated	4
Papillary	1
No descriptor/other	8
Poorly differentiated carcinoma	9
Squamous cell carcinoma	2
Unknown/other	4
No. of involved organ sites	**No. of patients**
1	12
2	4
3	7
4 or more	5

Table 3 Characteristics of 16 patients treated with the CDDP/TXT regimen

Characteristic	No. of Patients
Sex	
Female	6
Male	10
Age, years	
Median	62.5
Range	41–76
PS	
0–1	12
2–3	4
Histology	
Adonocarcinoma	10
Poorly differentiated	2
Papillary	1
No descriptor/other	7
Poorly differentiated Carcinoma	4
Squamous cell carcinoma	0
Unknown/other	2
Metastatic sites at presentation	
Lymph nodes	10
Bone	6
Lung	2
Liver	1
Pleura/pleural space	1
Peritoneum	2
Skin	1
Adrenal	1
Others	4
No. of involved organ sites	
Single site	9
Multiple (≥2) sites	7
No. of courses given	
Median	3
Range	1–6

characteristics were similar to those of all 28 patients (Table 3): 10 men and 6 women, median age 62.5 years (range 41–76 years). However, performance status (PS) and the number of metastatic sites were lower, with PS 0–1 in 12 patients and single-site involvement in 9. In 8 patients (50%), more than 2 tumor markers had increased at diagnosis. The median duration from the day of the pathological diagnosis of metastatic carcinoma to the first day of CDDP/TXT therapy was 43 days (range 0–154 days). A total of 44 cycles of therapy was given, and the patients underwent a median of 3 treatment cycles (range 1–6 cycles). Doses were modified mainly because of hematological toxicity; 4 patients had a 20% dose reduction.

The overall response rate was 62.5% (95% CI 8.6–81.5%), with CR in one patient and PR in nine patients. Six of 10 patients with adenocarcinoma responded, and all 4 patients with poorly differentiated carcinoma responded. Tumor markers decreased in most responding patients. Fig. 1 shows the survival curve for these patients. The median follow-up was 20.4 months (range 1.7–60.2 months), the median disease-free survival (DFS) was 8.7 months, the 1-year overall survival (OS) rate was 68.8% (95% CI 40.6–91.5%), and the median OS was 22.7 months. The median hospitalization stay of the 16 patients treated with CDDP/TXT therapy was 65.5 days (range 26–162 days).

Toxicity data are listed in Table 4. Grade 3–4 neutropenia was frequent (14 patients, 87.5%). One patient who had multiple lung, liver, and bone metastases died of bacterial pneumonia due to neutropenia. Hyponatremia occurred in 14 patients (87.5%) and was grade 3–4 in 3 patients; however, all patients were able to continue the treatment. The hyponatremia was caused by a loss of sodium due to renal tubule damage caused by cisplatin or the syndrome of inappropriate secretion of antidiuretic hormone (SIADH). Grade 3 allergic reactions due to docetaxel occurred in 2 patients during the first course. These 2 patients were given hydrocortisone and treated with cisplatin-only beginning with the next course. Other recorded toxicities were mild to moderate.

Prognostic factors for survival in the 28 patients with CUP. Fig. 2 shows the survival

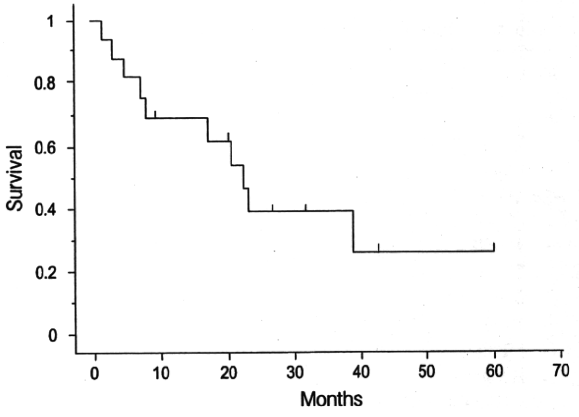

Fig. 1 Kaplan-Meier survival curve for the CUP patients treated with CDDP/TXT chemotherapy (n = 16).

curve for the 28 patients with CUP calculated from the day of diagnosis. The 1-year OS rate for all 28 patients was 45.6% (95% CI 26.8-64.4%), and the median survival was 8.3 months.

Table 5 lists the median survival of the CUP patient subgroups according to various factors. The univariate analysis revealed that 4 factors were deleterious: performance status 2-4, liver involvement, bone involvement, and pleural involvement. The advantageous clinical feature was lymph node involvement.

Discussion

In this study, we obtained an excellent response rate and survival with CDDP/TXT therapy for patients with CUP. An overall response rate of 62.5% was seen in patients with CUP who were given the CDDP/TXT combination once every 3 weeks. The median disease-free survival was 8.7 months. The 1-year OS was 68.8%, and the median OS was 22.7 months. The response rate and survival were superior to those obtained in the reported phase II trials of platinum plus taxane-based chemotherapy [2, 5, 6, 12]. Greco *et al.* reported a prospective phase II study of the CDDP/TXT regimen with a response rate of 22% and a 1-year survival of 40% [6]. The patient characteristics and dose intensity were similar to those in our study, although they had fewer patients with a single metastasis.

Yakushiji *et al.* have reported that 35 Japanese patients received a median of four cycles of CDDP and TXT, and had a response rate of 57.1%. The median survival time was 13.2 months [13]. These results in Japanese patients together with ours in the present study seem to be better than those reported from other countries. Although the prognostic factors in our reports are similar to those for other countries, Japanese patients with CUP might be chemosensitive and thus survive longer.

The treatment-related toxicity of the CDDP/TXT regimen mainly involved myelosuppression; in particular, grade 3-4 neutropenia was severe. Non-prophylactic G-CSF seemed to be the cause of this severity. One patient died of bacterial pneumonia due to neutropenia on day 12 of the first course. This patient was a 62-year-old man with PS 3. He had multiple metastases to lung, liver, and bone. He was therefore at high risk of pneumonia and had a very poor prognosis. Although hyponatremia occurred in 87.5% of our patients, it has not been reported in other studies that treated patients with CUP using platinum-containing regimens. Greco *et al.* have reported the toxicities of CDDP/TXT therapy to consist primarily of gastrointestinal events, with myelosuppression being moderate [6]. Based on urinalysis and the serum osmolarity, SIADH was the main cause of hyponatremia in the present study (data not shown). Since 1990, many Japanese researchers have reported SIADH following platinum administration for solid tumors [14, 15]. Collectively, Japanese patients seem to be more sensitive to platinum in terms of developing SIADH. Other recorded toxicities are mild to moderate. Overall, the regimen is generally tolerated in the majority of patients.

Table 4 Toxicity of CDDP/TXT therapy as worst grade per patient (n = 16)

Toxicity	No. of patients (%)			
	Grade 1	Grade 2	Grade 3	Grade 4
Anemia	6 (37.5)	6 (37.5)	1	0
Thrombocytopenia	4 (25.0)	1	0	1
Leukocytopenia	0	5 (31.3)	7 (43.8)	3 (18.8)
Granulocytopenia	0	1	3 (18.8)	11 (68.8)
Diarrhea	2 (12.5)	0	0	0
Nausea	3 (18.8)	5 (31.3)	4 (25.0)	0
Hyponatremia	11 (68.8)	0	3 (18.8)	0
High serum bilirubin	2 (12.5)	0	1	0
High serum creatinine	7 (43.8)	0	0	0
Allergic reaction	0	0	2 (12.5)	0

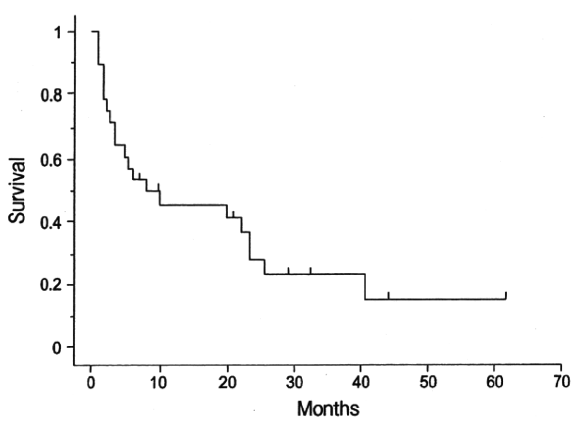

Fig. 2 Kaplan-Meier survival curve of all 28 CUP patients.

Table 5 Median survival duration of defined patient populations with CUP

Variable		No. of Patients	Median survival (days)	*p*-value
Sex				
Female		9	712	0.2599
Male		19	186	
No. of organ sites				
1		12	709	0.1180
2-6		16	108	
Performance status				
0-1		17	673	**0.0413**
2-3		11	79	
Involved organ sites				
Lymph nodes	+	18	673	**0.0310**
	−	10	148	
Liver	+	6	50	**0.0002**
	−	22	673	
Bone	+	10	108	**0.0380**
	−	18	673	
Lung	+	7	67	0.0642
	−	21	604	
Pleura/pleural space	+	4	31	**0.0040**
	−	24	604	
Brain	+	1	108	0.3704
	−	27	306	
Peritoneum	+	4	67	0.1458
	−	24	306	
Adrenal	+	2	33	0.6633
	−	26	249	
Skin	+	3	51	0.1820
	−	25	306	
Therapy				
CDDP/TXT		16	681	<0.0001
Other		12	73	
Histology				
Adenocarcinoma		13	673	
Poorly differentiated carcinoma		9	306	
Squamous cell carcinoma		2	33	
Unknown or others		4	67	

Clinical subsets of patients who are sensitive to platinum-containing treatment have been identified in the last 2 decades [2]. In this study, one patient almost fit into a favorable subset. She was a 73-year-old woman with peritoneal adenocarcinoma, but no papillary serous carcinoma, so she did not completely conform to a favorable subset. She was given three courses of CDDP/TXT, attained good PR, and was still alive at the 23.6-month follow-up. Therefore, although no patients completely matched the subgroups with a favorable prognosis, the CDDP/TXT regimen in this study was found to be very beneficial.

We also analyzed the course and prognostic factors of the patients with CUP. Univariate analysis identified 4 factors predicting a poor prognosis: performance status 2-4, liver involvement, bone involvement, and pleural involvement. The one favorable prognostic factor was lymph node involvement. Abbruzzese *et al.* examined prognostic factors in 657 consecutive patients and found that male sex, increased numbers of involved organ sites, adenocarcinoma histology, and hepatic involvement were negative prognostic factors in a multivariate analysis [16]. They also reported that lymph node involvement,

peritoneal involvement, and neuroendocrine histology are favorable prognostic factors [16]. Our results confirm the reported analyses; *i.e.*, visceral metastasis, multiple metastatic sites, and poor performance status may predict shorter survival.

Recently, a new combination of chemotherapy has been reported that includes gemcitabine, etoposide, or irinotecan combined with platinum plus taxane; these studies have shown similar response and survival rates [17, 18]. New agents such as vascular endothelial growth factor (VEGF) inhibitors and epidermal growth factor receptor (EGFR) inhibitors are being tested to improve the prognosis of CUP. Hainsworth *et al.* have reported that bevacizumab plus erlotinib therapy has a response rate of 10%, leading to stable disease in 61%, a median OS of 7.4 months, and a 1-year OS of 33% [19]. Therapeutic trials involving platinum and taxane plus VEGF or EGFR inhibitors should be conducted to improve the survival of patients with CUP.

In conclusion, although this was a retrospective study, we observed an excellent response rate and survival with CDDP/TXT chemotherapy in Japanese patients with CUP, despite their being in unfavorable subgroups. Our results show that bone, liver, and pleural metastasis, and poor performance status may predict a shorter survival.

References

1. Pavlidis N, Briasoulis E, Hainsworth J and Greco FA: Diagnostic and therapeutic management of cancer of an unknown primary. Eur J Cancer (2003) 39: 1990-2005.
2. Briasoulis E, Kalofonos H, Bafaloukos D, Samantas E, Fountzilas G, Xiros N, Skarlos D, Christodoulou C, Kosmidis P and Pavlidis N: Carboplatin plus paclitaxel in unknown primary carcinoma: A phase II hellenic cooperative oncology group study. J Clin Oncol (2000) 18: 3101-3107.
3. Culine S, Lortholary A, Voigt JJ, Bugat R, Theodore C, Priou F, Kaminsky MC, Lesimple T, Pivot X, Coudert B, Douillard JY, Merrouche Y, Allouache J, Goupil A, Negrier S, Viala J, Petrow P, Bouzy J, Laplanche A and Fizazi K: Cisplatin in combination with either gemcitabine or irinotecan in carcinomas of unknown primary site: Results of a randomized phase II study--trial for the French Study Group on Carcinomas of Unknown Primary (gefcapi 01). J Clin Oncol (2003) 21: 3479-3482.
4. Guardiola E, Pivot X, Tchicknavorian X, Magne N, Otto J, Thyss A and Schneider M: Combination of cisplatin-doxorubicin-cyclophosphamide in adenocarcinoma of unknown primary site: A phase II trial. Am J Clin Oncol (2001) 24: 372-375.
5. Mukai H, Watanabe T, Ando M and Katsumata N: Unknown primary carcinoma: A feasibility assessment of combination chemotherapy with cisplatin and docetaxel. Int J Clin Oncol (2003) 8: 23-25.
6. Greco FA, Erland JB, Morrissey LH, Burris HA 3rd, Hermann RC, Steis R, Thompson D, Gray J and Hainsworth JD: Carcinoma of unknown primary site: Phase II trials with docetaxel plus cisplatin or carboplatin. Ann Oncol (2000) 11: 211-215.
7. Miller AB, Hoogstraten B, Staquet M and Winkler A: Reporting results of cancer treatment. Cancer (1981) 47: 207-214.
8. Trotti A, Colevas AD, Setser A, Rusch V, Jaques D, Budach V, Langer C, Murphy B, Cumberlin R, Coleman CN and Rubin P: CTCAE v3.0: Development of a comprehensive grading system for the adverse effects of cancer treatment. Semin Radiat Oncol (2003) 13: 176-181.
9. Kaplan D: Pseudocyst of the pancreas. Am J Surg (1958) 95: 160-162.
10. Mantel N: Evaluation of survival data and two new rank order statistics arising in its consideration. Cancer Chemother Rep (1966) 50: 163-170.
11. Oken MM, Creech RH, Tormey DC, Horton J, Davis TE, McFadden ET and Carbone PP: Toxicity and response criteria of the eastern cooperative oncology group. Am J Clin Oncol (1982) 5: 649-655.
12. Park YH, Ryoo BY, Choi SJ, Yang SH and Kim HT: A phase ii study of paclitaxel plus cisplatin chemotherapy in an unfavourable group of patients with cancer of unknown primary site. Jpn J Clin Oncol (2004) 34: 681-685.
13. Yakushiji S, Ando M, Yonemori K, Kohno T, Shimizu C, Katsumata N and Fujiwara Y: Cancer of unknown primary site: Review of consecutive cases at the national cancer center hospital of japan. Int J Clin Oncol (2006) 11: 421-425.
14. Yokoyama Y, Shigeto T, Futagami M and Mizunuma H: Syndrome of inappropriate secretion of anti-diuretic hormone following carboplatin-paclitaxel administration in a patient with recurrent ovarian cancer. Eur J Gynaecol Oncol (2005) 26: 531-532.
15. Kagawa K, Fujitaka K, Isobe T, Yamasaki M, Miyazaki M, Oguri T and Kohno N: Syndrome of inappropriate secretion of ADH (SIADH) following cisplatin administration in a pulmonary adenocarcinoma patient with a malignant pleural effusion. Intern Med (2001) 40: 1020-1023.
16. Abbruzzese JL, Abbruzzese MC, Hess KR, Raber MN, Lenzi R and Frost P: Unknown primary carcinoma: Natural history and prognostic factors in 657 consecutive patients. J Clin Oncol (1994) 12: 1272-1280.
17. Hainsworth JD, Erland JB, Kalman LA, Schreeder MT and Greco FA: Carcinoma of unknown primary site: Treatment with 1-hour paclitaxel, carboplatin, and extended-schedule etoposide. J Clin Oncol (1997) 15: 2385-2393.
18. Greco FA, Burris HA 3rd, Litchy S, Barton JH, Bradof JE, Richards P, Scullin DC Jr, Erland JB, Morrissey LH and Hainsworth JD: Gemcitabine, carboplatin, and paclitaxel for patients with carcinoma of unknown primary site: A minnie pearl cancer research network study. J Clin Oncol (2002) 20: 1651-1656.
19. Hainsworth JD, Spigel DR, Farley C, Thompson DS, Shipley DL and Greco FA: Phase II trial of bevacizumab and erlotinib in carcinomas of unknown primary site: The minnie pearl cancer research network. J Clin Oncol (2007) 25: 1747-1752.

Combination of morphological feature analysis and immunohistochemistry is useful for screening of EML4-ALK-positive lung adenocarcinoma

Ryu Jokoji,[1] Takashi Yamasaki,[1] Seigo Minami,[2] Kiyoshi Komuta,[2] Yasushi Sakamaki,[3] Kengo Takeuchi,[4] Masahiko Tsujimoto[1]

[1]Department of Pathology, Osaka Police Hospital, Tennouji-ku, Osaka, Japan
[2]Department of Respiratory Medicine, Osaka Police Hospital, Tennouji-ku, Osaka, Japan
[3]Department of Chest Surgery, Osaka Police Hospital, Tennouji-ku, Osaka, Japan
[4]Division of Pathology, The Cancer Institute, Japanese Foundation for Cancer Research, Ariake, Koto-ku, Tokyo, Japan

Correspondence to
Masahiko Tsujimoto, Department of Pathology, Osaka Police Hospital, 10–31 Kitayama-cho, Tennouji-ku, Osaka 543-0035, Japan; patho@oph.gr.jp

Accepted 27 August 2010
Published Online First 9 October 2010

ABSTRACT

Background A subset of lung cancers harbours the fusion gene echinoderm microtubule-associated protein-like-4—anaplastic lymphoma kinase (EML4-ALK). Recently, immunohistochemistry for ALK has shown sensitivity for the detection of EML4-ALK-positive lung adenocarcinoma almost equal to that of the fluorescence in situ hybridisation (FISH) assay.

Aims To study the clinicopathological features of EML4-ALK-positive lung adenocarcinoma in a large number of surgically resected samples using immunohistochemistry, in order to establish a useful screening method for EML4-ALK-positive lung adenocarcinoma.

Methods Immunohistochemistry for ALK was used to screen for EML4-ALK-positive lung adenocarcinomas in 254 cases of surgically resected samples.

Results EML4-ALK-positive cases were detected in 3.1% of lung adenocarcinomas (8/254). EML4-ALK-positive lung adenocarcinomas showed significant associations with intra- and/or extra-cytoplasmic mucin ($p=0.0001$), and cribriform pattern with excessive extracytoplasmic mucin ($p<0.0001$). Signet-ring cell appearance alone lacked significance ($p=0.149$).

Conclusion EML4-ALK-positive lung adenocarcinoma has a tendency to express a characteristic morphological pattern. The combined use of morphological feature analysis and immunohistochemistry may be a useful and cost effective screening method for EML4-ALK lung adenocarcinoma.

INTRODUCTION

Lung cancer is the major cause of cancer-related deaths in the world. It is known that some gene mutations are involved in carcinogenesis of the lung. Epidermal growth factor receptor (EGFR) is an example of a gene mutation in lung cancer. Activation of the mutation in EGFR defines a group of patients with sensitivity to the chemical inhibitor for the kinase activity of EGFR, accounting for about 10% of primary lung cancers.[1 2] In 2007, Soda *et al* identified the fusion oncogene joining the echinoderm microtubule-associated protein-like-4 (EML4) and the anaplastic lymphoma kinase gene (ALK) in non-small-cell lung cancer (NSCLC).[3] The detection of EML4-ALK-positive lung cancer is needed to identify lung cancer patients for molecular target therapy. Some authors recommend molecular cascade screening for the detection of EML4-ALK-positive lung cancer.[4] The cascade is a stepwise approach to test for gene mutations in lung adenocarcinoma: first for KRAS, second for EGFR, and third for EML4-ALK translocation. However, it is an expensive and time-consuming method. Moreover, EML4-ALK-positive lung cancer accounts for only about 5% of all NSCLC patients according to previous reports.[3 5–8] To find a more efficient screening method for EML4-ALK-positive lung cancer, more precise clinical features and histopathological findings of EML4-ALK-positive lung cancer must be determined.

A previous report showed that EML4-ALK-positive lung cancers are characterised by smaller tumour size, and found in younger patients who are non-smokers or light smokers.[6] Another study reported that EML4-ALK-positive lung cancer showed acinar morphology[9] and signet-ring cell appearance.[5 10]

Recently, immunohistochemistry for ALK has shown sensitivity for the detection of EML4-ALK-positive lung adenocarcinoma almost equal to that of the fluorescence in situ hybridisation (FISH) assay.[11] In this study, the clinicopathological features of EML4-ALK-positive lung adenocarcinoma were studied in a large number of surgically resected samples using immunohistochemistry, in order to establish a useful screening method for EML4-ALK-positive lung adenocarcinoma.

MATERIALS AND METHODS

Patients and sample collection

This study included samples from 254 Japanese NSCLC patients with a diagnosis of lung adenocarcinoma who underwent surgery at Osaka Police Hospital (Osaka, Japan) between January 2000 and December 2009. Clinical data were collected from inpatient and outpatient medical records.

Histological analysis

All surgically resected lung tumour specimens were embedded in paraffin and serial 5 μm thick sections were prepared. The pathological examination was based on standard H&E stained slides from all blocks of tissues. Pathological stage and differentiation were evaluated according to the current international tumour node metastasis (TNM) staging system and the World Health Organization classification. All tumour slides (consisting in each case of 1–25 slides, with a mean of six slides) were reviewed, and classified according to WHO histological types. In this study, bronchioloalveolar carcinoma is a pure type of carcinoma without invasion. The mixed subtypes category contained varied lesions. Therefore, in this study, an

J Clin Pathol 2010;**63**:1066–1070. doi:10.1136/jcp.2010.081166

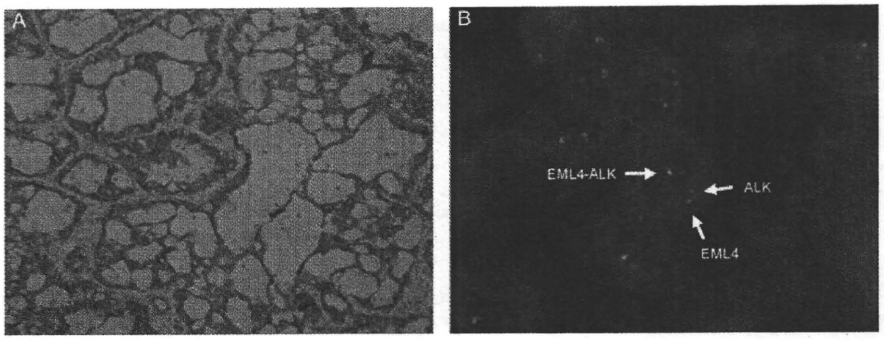

Figure 1 (A) Anaplastic lymphoma kinase (ALK) protein was expressed in the cytoplasm with no nuclear staining. (B) Fluorescence in situ hybridisation assay of echinoderm microtubule-associated protein-like-4—ALK.

additional predominance classification was used, as described in a previous report.[6] Regardless of percentage, the most dominant subtype was regarded as the predominant subtype. The remaining subtypes were regarded as minor components.

Three pathologists (RJ, TY, MT) reviewed all tumour slides of all cases. The decision on discrepant cases was made by consensus when two of the three pathologists agreed. All discrepant cases (10 cases) resulted in consensus.

Immunohistochemical analysis

Unstained paraffin-embedded sections were deparaffinised in xylene, hydrated through and rinsed in distilled water. Heat-induced epitope retrieval was performed with EnVision FLEX Target Retrieval Solution, High pH (Dako, Carpinteria, California, USA). Slides were then incubated at room temperature with antibody to ALK (clone 5A4, 1:100, Abcam) for 30 min. To increase the sensitivity of detection, the intercalated antibody-enhanced polymer (iAEP) method was used with minor modifications.[12] Slides were incubated at room temperature with EnVision FLEX+ Mouse Linker (Dako) for 15 min. The immune complexes were then detected with the dextran polymer reagent.

Table 1 Clinicopathological comparison between echinoderm microtubule-associated protein-like-4—anaplastic lymphoma kinase (EML4-ALK)-positive and -negative lung adenocarcinoma

	(n=254)	EML4-ALK (+) (n=8)	EML4-ALK (−) (n=246)	p Value
Age	Mean±SD	61.75±11.41	66.55±9.246	0.1524*
	Median	65.5	67.5	
	Range	44–77	42–87	
Sex	Male	4	126	1‡
	Female	4	120	
Smoking habit	Never smoker	2	49	0.114†
	Ever smoker	5	79	
	Unknown	1	118	
Tumour size (mm)	Mean±SD	25.88±10.3	23.58±11.65	0.581*
	Median	26.5	21	
	Range	10–45	5–75	
Differentiation	Well (G1)	0	132	0.0025‡
	Less (G2, G3)	8	114	(G1 vs G2, G3)
Tumour status	pT1	6	169	1‡ (pT1 vs T2-4)
	pT2–pT4	2	77	
Lymph node metastasis	pN0	4	193	0.0782‡ (pN0 vs pN1-3)
	pN1–3	4	53	
TNM stage	pStage I	4	175	0.2403‡ (pStage I vs pStage II–IV)
	pStage II–IV	4	71	
EGFR mutation (n=67)	(+)	0	33	
	(−)	8	26	

*Student's t test b.
†χ^2 test.
‡Fisher's exact test.
EGFR, epidermal growth factor receptor.

FISH assay

FISH was performed on formalin-fixed paraffin-embedded tumour tissues with use of fluorescently-labelled bacterial artificial chromosome clone probes specific to the ALK and the EML4 loci (EML4 RP11-996L7; ALK RP11-984I21, RP11-62B19) using a histology FISH accessory kit (Dako).

DNA extraction and mutation analysis of EGFR, KRAS

Because no fresh sample was available for this study, DNA was extracted from formalin-fixed paraffin-embedded tissues; mutations in the EGFR (exons 18–21) genes were analysed by the peptide nucleic acid locked nucleic acid PCR-clamp (PNA LNA PCR-clamp) technique[13] and in the KRAS (codons 12,13) genes by direct sequencing.[14] Mutation analysis was performed on 67 cases, for which informed consent was obtained from patients. The ethics committee of our institute approved the genetic analyses in the present study.

Statistical analysis

Statistical analysis for the tumour size and age was carried out using Student's t test. The values are shown as mean ± SD. The relationship between EML4-ALK expression and clinicopathological variables was analysed with the χ^2 test or Fisher's exact test. Statistical significance was defined as $p<0.05$.

RESULTS

Clinical presentation

Using immunohistochemistry for ALK, the expression of ALK was studied in 254 lung adenocarcinomas. Eight of 254 cases showed homogeneous ALK protein in the cytoplasm without nuclear staining. The percentage of positive tumour cells ranged from 80% to 100%. Varied intensity of ALK expression was observed. The FISH assay confirmed the presence of the EML4-ALK fusion gene in the eight cases that showed the ALK protein (figure 1).

Table 1 summarises details of the clinicopathological features of all cases. All patients were Japanese, ranging in age from 42 to 87 years, with a mean age of 66.4 years. The maximum diameter of their tumours ranged from 0.5 to 7.5 cm. EML4-ALK-positive

lung adenocarcinomas were significantly less differentiated than the EML4-ALK-negative lung adenocarcinomas (p=0.0025). EML4-ALK-positive and EML4-ALK-negative lung adenocarcinomas showed no difference in age, sex, tumour size, smoking habit and TNM stage. However, EML4-ALK-positive lung adenocarcinomas showed a tendency for association with younger patients, positive lymph nodes, adverse pathological stage and smoking habit. All of the EML4-ALK-positive cases had no mutation of the EGFR and KRAS genes.

Pathological findings and immunohistochemistry

Histologically, the 254 adenocarcinomas were comprised of 153 mixed subtypes, 34 acinar, 30 papillary, 2 others and 35 bronchioloalveolar carcinomas based on the WHO classification. The mixed subtypes category contained varied lesions. Therefore an additional predominance classification was used, as described in a previous report.[6] According to the predominance subtyping, the 254 adenocarcinomas were comprised of 85 acinar, 83 papillary, 74 bronchioloalveolar non-mucinous carcinomas, 7 bronchioloalveolar mucinous carcinomas and 5 others (table 2).

Table 2 also summarises the histological features of all cases. According to the predominance subtypes, six of eight EML4-ALK-positive lung adenocarcinomas (75%) were subclassified as acinar-predominant adenocarcinomas and the other two cases were papillary-predominant adenocarcinomas. When compared with EML4-ALK-negative lung adenocarcinoma, the association of EML4-ALK-positive lung adenocarcinoma and acinar morphology was statistically significant (p=0.0184, Fisher's exact test). In other words, six of 85 (7.0%) acinar-predominant adenocarcinomas were positive for EML4-ALK fusion.

Lung adenocarcinoma cells have intracytoplasmic mucin in varying degrees and sometimes have extracytoplasmic mucin. Some lung adenocarcinoma cells show signet-ring cell like appearance because of excessive intracytoplasmic mucin (figure 2). Also, other lung adenocarcinomas show a cribriform pattern with excessive extracytoplasmic mucin (figure 3). In the 254 cases examined, 36 had intracytoplasmic or extracytoplasmic mucin detected by Alcian blue stain.

Table 2 Subtypes by predominance classification

	Total	EML4-ALK (+)	EML4-ALK (−)
	254	8 (3.1%)	246
Papillary	83	2	81
Acinar	85	6	79*
Bronchioloalveolar carcinoma, non-mucinous	74	0	74
Bronchioloalveolar carcinoma, mucinous	7	0	7
Others	5	0	5

*Fisher's exact test, p=0.0184 (acinar predominant adenocarcinoma vs the other adenocarcinoma).
EML4-ALK, echinoderm microtubule-associated protein-like-4—anaplastic lymphoma kinase.

EML4-ALK-positive lung adenocarcinomas showed significant associations with intra- and/or extra-cytoplasmic mucin (p=0.0001), and cribriform pattern with excessive extracytoplasmic mucin (p<0.0001). Signet-ring cell appearance alone lacked significance (p=0.149) (table 3).

Two of eight EML4-ALK-positive cases did not have a characteristic morphological feature, nor did they show any mucin production (tables 4 and 5).

DISCUSSION

A large-scale screening conducted for EML4-ALK-positive lung adenocarcinomas in our institute detected eight cases. In this study, the association of EML4-ALK-positive lung adenocarcinoma and acinar-predominant morphology, extra- and/or intracytoplasmic mucin production and cribriform pattern with excessive extracytoplasmic mucin was demonstrated. A previous report showed that EML4-ALK-positive lung cancers were characterised by smaller tumour size, younger patients and non-smokers or light smokers when compared against

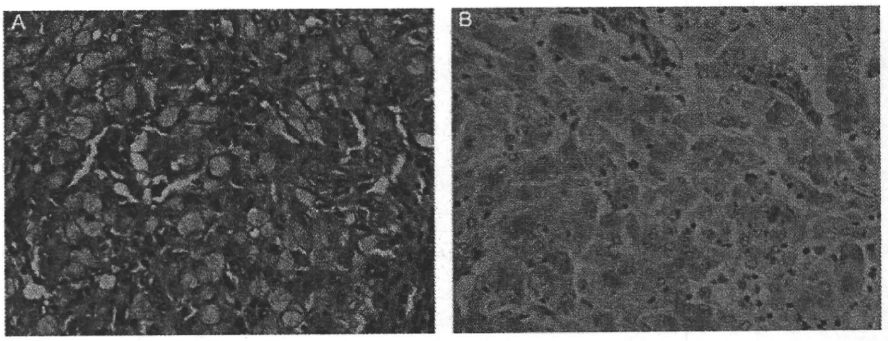

Figure 2 (A) Echinoderm microtubule-associated protein-like-4—anaplastic lymphoma kinase (EML4-ALK)-positive lung adenocarcinoma cells showing signet-ring cell like appearance because of excessive intracytoplasmic mucin. (B) Alcian blue staining showing excessive intracytoplasmic mucin.

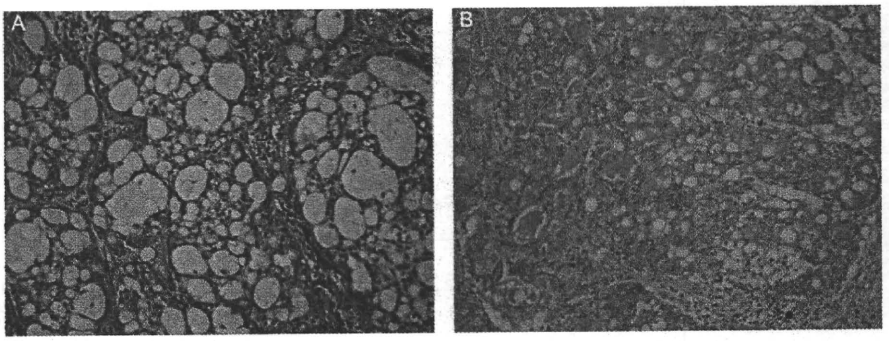

Figure 3 (A) Echinoderm microtubule-associated protein-like-4—anaplastic lymphoma kinase (EML4-ALK)-positive lung adenocarcinoma showing cribriform pattern with excessive extracytoplasmic mucin. (B) Alcian blue staining showing excessive extracytoplasmic mucin.

J Clin Pathol 2010;63:1066–1070. doi:10.1136/jcp.2010.081166

Table 3 Histological feature comparison between echinoderm microtubule-associated protein-like-4—anaplastic lymphoma kinase (EML4-ALK)-positive and -negative lung adenocarcinoma

		EML4-ALK (+)	EML4-ALK (−)	p Value*
Extra- and/or intra-cytoplasmic mucin production	(+)	6	30	0.0001
	(−)	2	216	
Cribriform pattern with extracytoplasmic mucin	(+)	5	8	<0.0001
	(−)	3	238	
Signet-ring cell appearance	(+)	1	4	0.149
	(−)	7	242	

*Fisher's exact test.

EML4-ALK-negative lung cancers.[5 6 10 15] In this study EML4-ALK-positive lung adenocarcinoma was less differentiated, as described in a previous report.[6] However, EML4-ALK-positive and -negative lung adenocarcinomas showed no difference in age, sex, tumour size, smoking habit and TNM stage. The screening was limited in this study to lung adenocarcinomas of Japanese patients. Previous reports showed that lung cancers harbouring the EML4-ALK fusion gene were mostly adenocarcinomas with a few exceptions.[10 15] All EML4-ALK-positive lung adenocarcinomas had no mutation in the EGFR and KRAS genes, which concurred with previous reports.[6 9 15]

A previous report revealed the association of EML4-ALK fusion and acinar-predominant morphology[9] and signet-ring cell appearance.[5 10] In this study, acinar-predominant morphology and cribriform pattern with excessive extracytoplasmic mucin were useful factors, suggesting the presence of the EML4-ALK fusion gene, but signet-ring cell appearance by itself was not a useful factor. Previous reports revealed an association of EML4-ALK fusion and signet-ring cell appearance. However, the subjects screened were in a Western population or with limited clinical characteristics.[5 10] There may be an underlying difference in the subject population by race and clinical characteristics. A recent report showed that primary signet-ring cell carcinoma of the lung shares many clinicopathologic characteristics with EML4-ALK-positive lung cancers.[16] In point of fact, one case of EML4-ALK-positive lung adenocarcinoma in our study had signet-ring cell appearance. However, because the population of tumour cells appearing like signet-ring cells was very low, it was not a useful independent factor, suggesting the presence of the EML4-ALK fusion gene. It may however, be a clue in suggesting the presence of the EML4-ALK fusion gene because of excessive mucin production.

Previous reports have shown the utility of immunohistochemistry for EML4-ALK.[11 12] Our study showed the usefulness of characteristic morphological features in screening for EML4-ALK-positive lung adenocarcinomas. The combined study of typical morphological features of EML4-ALK-positive lung adenocarcinomas by light microscopy followed by immunohistochemical confirmation may enable the screening for EML4-ALK-positive lung adenocarcinomas to be simple and cost effective.

Although light microscopic observations of specific morphological features and immunohistochemistry are very useful, two of our eight EML4-ALK-positive cases did not have characteristic morphological features. The two cases showed acinar-

Table 4 Clinical features of echinoderm microtubule-associated protein-like-4—anaplastic lymphoma kinase (EML4-ALK)-positive lung adenocarcinoma

Case no.	Age (y)	Sex	Smoking habit	Tumour size (mm)*	EGFR mutation	KRAS mutation	Lymph node metastasis	pStage	Prognosis
1	46	F	Never	16	(−)	(−)	Negative	IA	AN (11 mth)
2	64	M	Ever	45	(−)	(−)	Negative	IB	Recurrence at 12 mth alive (23 mth)
3	44	M	Ever	25	(−)	(−)	Positive (pN2)	IIIA	Recurrence at 29 mth alive (42 mth)
4	67	F	Never	28	(−)	(−)	Positive (pN1)	IIA	Recurrence at 20 mth alive (39 mth)
5	60	F	Ever	28	(−)	(−)	Negative	IA	AN (15 mth)
6	77	M	Ever	25	(−)	(−)	Negative	IA	AN (11 mth)
7	67	F	Unknown	10	(−)	(−)	Positive (pN2)	IIIA	DD (12 mth)
8	69	M	Ever	30	(−)	(−)	Positive (pN1)	IIA	DD (43 mth)

*Size is represented by the maximum width of the neoplasm.
AN indicates patient is alive with no evidence of disease; DD, died from disease; acinar, acinar adenocarcinoma; papillary, papillary adenocarcinoma; mixed, adenocarcinoma with mixed subtypes.
pStage, pathological stage; EGFR, epidermal growth factor receptor.

Table 5 Pathological features of echinoderm microtubule-associated protein-like-4—anaplastic lymphoma kinase (EML4-ALK)-positive lung adenocarcinoma

Case no.	WHO subtype	Predominant subtype	Minor component subtypes	ALK positive tumour cells (%)	Mucin production	Cribriform pattern	Signet-ring cell appearance
1	Mixed	Acinar	Papillary	100	(+)	(+)	(−)
2	Mixed	Papillary	Acinar	90	(+)	(+)	(−)
3	Acinar	Acinar	–	100	(+)	(+)	(−)
4	Acinar	Acinar	–	80	(+)	(+)	(−)
5	Mixed	Acinar	Solid	100	(+)	(−)	(+)
6	Mixed	Papillary	BAC, acinar, micropapillary	100	(+)	(+)	(−)
7	Acinar	Acinar	–	100	(−)	(−)	(−)
8	Acinar	Acinar	–	100	(−)	(−)	(−)

Mixed indicates adenocarcinoma with mixed subtypes; acinar, acinar adenocarcinoma; papillary, papillary adenocarcinoma; mixed, adenocarcinoma with mixed subtypes; solid, solid adenocarcinoma with mucin production; BAC, bronchioloalveolar carcinoma, non-mucinous; micropapillary, micropapillary carcinoma; mucin production, extra- and/or intra-cytoplasmic mucin production; histological pattern, specific histological pattern; cribriform, cribriform pattern with excessive extracytoplasmic mucin; signet-ring cell, signet-ring cell appearance.

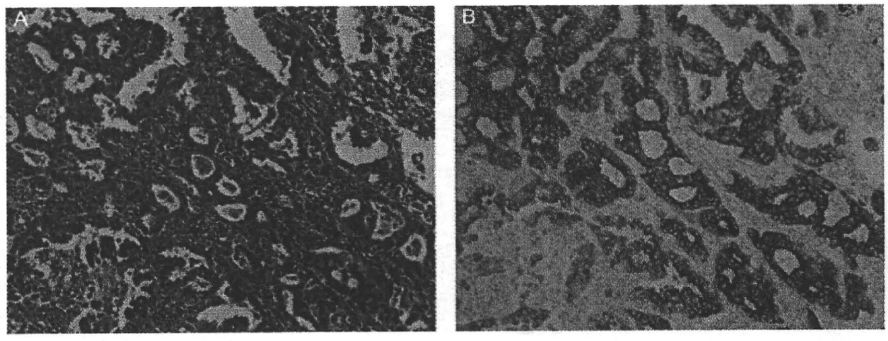

Figure 4 (A) One echinoderm microtubule-associated protein-like-4—anaplastic lymphoma kinase (EML4-ALK)-positive lung adenocarcinoma showing acinar pattern without mucin production. (B) ALK protein was expressed in the cytoplasm with no nuclear stain.

Take-home messages

- EML4-ALK-positive lung adenocarcinomas were significantly less differentiated than the EML4-ALK-negative lung adenocarcinomas.
- EML4-ALK-positive lung adenocarcinomas showed significant associations with intra- and/or extra-cytoplasmic mucin, and cribriform pattern with excessive extracytoplasmic mucin.
- The combined study of typical morphological features of EML4-ALK-positive lung adenocarcinomas by light microscopy followed by immunohistochemical confirmation may enable the screening for EML4-ALK-positive lung adenocarcinomas to be simple and cost effective.

predominant morphology but no mucin production (figure 4 and table 5). A large-scale, multi-institute study will be needed to offer more insight into EML4-ALK-positive lung adenocarcinomas.

In this study, the FISH assay was performed only on positive cases. Standard methods are not yet established for detection of the EML4-ALK fusion gene in lung cancers. As previous reports showed,[5 17] both FISH and immunohistochemistry may have false negative results. However, to perform the FISH assay on all screening cases at any institute is a costly undertaking. Immunohistochemistry, on the other hand, has been used widely in the diagnostic laboratory. It is easy to perform and relatively inexpensive. Recently, immunohistochemistry for ALK has shown almost equal sensitivity to that of the FISH assay for the detection of EML4-ALK-positive lung adenocarcinomas.[11] In addition, the ALK fusion genes are recently discovered oncogenes in lung cancers. Conceivably, there is an unknown fusion partner of ALK, which cannot be detected by the FISH assay. Therefore, immunohistochemistry appears to be an appropriate screening method in the diagnostic laboratory.

In conclusion, we showed that EML4-ALK-positive lung adenocarcinomas had a tendency for expressing a characteristic morphological pattern. Continued investigations await the validation of the results presented in this study with respect to the potential usefulness of morphological analysis and immunohistochemistry in screening for EML4-ALK lung adenocarcinomas.

Acknowledgements The authors thank Drs Eiichi Morii and Ayumi Furumoto for helpful advice and discussion, and Mr Michihiko Noguchi, Ms Ayumi Tsukiyama, Mr Yasuhiro Hashimoto, Ms Kumi Tanaka and Ms Saori Fukuda for technical assistance.

Competing interests None.

Ethics approval This study was conducted with the approval of the ethics committee of Osaka Police Hospital.

Provenance and peer review Not commissioned; externally peer reviewed.

REFERENCES

1. **Paez JG,** Janne PA, Lee JC, *et al*. EGFR mutations in lung cancer: correlation with clinical response to gefitinib therapy. *Science* 2004;**304**:1497—500.
2. **Lynch TJ,** Bell DW, Sordella R, *et al*. Activating mutations in the epidermal growth factor receptor underlying responsiveness of non-small-cell lung cancer to gefitinib. *N Engl J Med* 2004;**350**:2129—39.
3. **Soda M,** Choi YL, Enomoto M, *et al*. Identification of the transforming EML4-ALK fusion gene in non-small-cell lung cancer. *Nature* 2007;**448**:561—6.
4. **Horn L,** Pao W. EML4-ALK: honing in on a new target in non-small-cell lung cancer. *J Clin Oncol* 2009;**27**:4232—5.
5. **Rodig SJ,** Mino-Kenudson M, Dacic S, *et al*. Unique clinicopathologic features characterize ALK-rearranged lung adenocarcinoma in the western population. *Clin Cancer Res* 2009;**15**:5216—23.
6. **Inamura K,** Takeuchi K, Togashi Y, *et al*. EML4-ALK lung cancers are characterized by rare other mutations, a TTF-1 cell lineage, an acinar histology, and young onset. *Mod Pathol* 2009;**22**:508—15.
7. **Takeuchi K,** Choi YL, Soda M, *et al*. Multiplex reverse transcription-PCR screening for EML4-ALK fusion transcripts. *Clin Cancer Res* 2008;**14**:6618—24.
8. **Rikova K,** Guo A, Zeng Q, *et al*. Global survey of phosphotyrosine signaling identifies oncogenic kinases in lung cancer. *Cell* 2007;**131**:1190—203.
9. **Inamura K,** Takeuchi K, Togashi Y, *et al*. EML4-ALK fusion is linked to histological characteristics in a subset of lung cancers. *J Thorac Oncol* 2008;**3**:13—17.
10. **Shaw AT,** Yeap BY, Mino-Kenudson M, *et al*. Clinical features and outcome of patients with non-small-cell lung cancer who harbor EML4-ALK. *J Clin Oncol* 2009;**27**:4247—53.
11. **Mino-Kenudson M,** Chirieac LR, Law K, *et al*. A novel, highly sensitive antibody allows for the routine detection of ALK-rearranged lung adenocarcinomas by standard immunohistochemistry. *Clin Cancer Res* 2010;**16**:1561—71.
12. **Takeuchi K,** Choi YL, Togashi Y, *et al*. KIF5B-ALK, a novel fusion oncokinase identified by an immunohistochemistry-based diagnostic system for ALK-positive lung cancer. *Clin Cancer Res* 2009;**15**:3143—9.
13. **Nagai Y,** Miyazawa H, Huqun, *et al*. Genetic heterogeneity of the epidermal growth factor receptor in non-small cell lung cancer cell lines revealed by a rapid and sensitive detection system, the peptide nucleic acid-locked nucleic acid PCR clamp. *Cancer Res* 2005;**65**:7276—82.
14. **Tam IY,** Chung LP, Suen WS, *et al*. Distinct epidermal growth factor receptor and KRAS mutation patterns in non-small cell lung cancer patients with different tobacco exposure and clinicopathologic features. *Clin Cancer Res* 2006;**12**:1647—53.
15. **Wong DW,** Leung EL, So KK, *et al*. The EML4-ALK fusion gene is involved in various histologic types of lung cancers from nonsmokers with wild-type EGFR and KRAS. *Cancer* 2009;**115**:1723—33.
16. **Ou SH,** Ziogas A, Zell JA. Primary signet-ring carcinoma (SRC) of the lung: a population-based epidemiologic study of 262 cases with comparison to adenocarcinoma of the lung. *J Thorac Oncol* 2010;**5**:420—7.
17. **Martelli MP,** Sozzi G, Hernandez L, *et al*. EML4-ALK rearrangement in non-small cell lung cancer and non-tumor lung tissues. *Am J Pathol* 2009;**174**:661—70.

Human Cancer Biology
See commentary p. 4909

Clinical Cancer Research

EML4-ALK Fusion Gene Assessment Using Metastatic Lymph Node Samples Obtained by Endobronchial Ultrasound-Guided Transbronchial Needle Aspiration

Yuichi Sakairi[1,7], Takahiro Nakajima[1,2,7], Kazuhiro Yasufuku[2], Dai Ikebe[3], Hajime Kageyama[4], Manabu Soda[5], Kengo Takeuchi[6], Makiko Itami[3], Toshihiko Iizasa[1], Ichiro Yoshino[7], Hiroyuki Mano[5], and Hideki Kimura[1]

Abstract

Purpose: Anaplastic lymphoma kinase (*ALK*) fusion genes represent novel oncogenes for non–small cell lung cancers (NSCLC). Several *ALK* inhibitors have been developed, and are now being evaluated in *ALK*-positive NSCLC. The feasibility of detecting *ALK* fusion genes in samples obtained by endobronchial ultrasound-guided transbronchial needle aspiration (EBUS-TBNA) was determined. The clinicopathologic characteristics of *ALK*-positive lung cancer were also analyzed.

Experimental Design: From April 2008 to July 2009, NSCLC cases with hilar/mediastinal lymph node metastases detected by EBUS-TBNA were enrolled. Positive expression of *ALK* fusion protein was determined using immunohistochemistry, and *ALK* gene rearrangements were further examined to verify the translocation between *ALK* and partner genes using fluorescent *in situ* hybridization and reverse transcription-PCR. Direct sequencing of PCR products was performed to identify *ALK* fusion variants.

Results: One hundred and nine cases were eligible for the analysis using re-sliced samples. Screening of these specimens with immunohistochemistry revealed *ALK* positivity in seven cases (6.4%), all of which possessed echinoderm microtubule–associated protein-like 4–*ALK* fusion genes as detected by fluorescent *in situ* hybridization and reverse transcription-PCR. All *ALK*-positive cases had an adenocarcinoma histology and possessed no *EGFR* mutations. Compared with *ALK*-negative cases, *ALK*-positive cases were more likely to have smaller primary tumors ($P < 0.05$), to occur at a younger age (<60 years; $P < 0.05$), and to occur in never/light smokers (smoking index < 400; $P < 0.01$). Mucin production was frequently observed in *ALK*-positive adenocarcinomas (29.4%; $P < 0.01$).

Conclusions: EBUS-TBNA is a practical and feasible method for obtaining tissue from mediastinal and hilar lymph nodes that can be subjected to multimodal analysis of *ALK* fusion genes in NSCLC.
Clin Cancer Res; 16(20); 4938–45. ©2010 AACR.

A small inversion within the short arm of human chromosome 2 leads to the generation of a fusion gene between the anaplastic lymphoma kinase (*ALK*) gene and the echinoderm microtubule–associated protein-like 4 (*EML4*) gene, the protein product of which is reported to function as an oncokinase in non–small cell lung cancer (NSCLC); in fact, this was the first oncogenic translocation to be identified in lung cancer (1). The *EML4-ALK* fusion gene has been detected in ~5% of NSCLC cases, and several *ALK* fusion gene variants have been reported (2). Standard methods for the detection of *ALK* fusion genes include reverse transcription-PCR (RT-PCR) with primers flanking the fusion points, as well as fluorescent *in situ* hybridization (FISH). Previously, immunohistochemistry-based diagnosis of *ALK* fusion genes in lung cancer has proven to be difficult, most likely due to the low expression level of the fusion protein products (3). An intercalated antibody-enhanced polymer (iAEP) technique has recently been developed that enables reliable immunohistochemistry-based detection of *ALK* fusion products (4). However, this technique has only been performed in cell lines and in large, surgically resected specimens; thus, it remains unclear whether such methodology can be applied to small biopsy samples obtained from patients with advanced NSCLC.

Endobronchial ultrasound-guided transbronchial needle aspiration (EBUS-TBNA) is an established modality for the definitive diagnosis of mediastinal and hilar adenopathy in

Authors' Affiliations: [1]Division of Thoracic Diseases, Chiba Cancer Center, Chiba, Japan; [2]Division of Thoracic Surgery, Toronto General Hospital, University Health Network, University of Toronto, Canada; [3]Division of Surgical Pathology, Chiba Cancer Center, Chiba, Japan; [4] Division of Genetic Diagnosis, Chiba Cancer Center, Chiba, Japan; [5]Division of Functional Genomics, Jichi Medical University, Tochigi, Japan; [6]Division of Pathology, The Cancer Institute, Japanese Foundation for Cancer Research, Tokyo, Japan; and [7]Department of General Thoracic Surgery, Graduate School of Medicine, Chiba University, Chiba, Japan

Corresponding Author: Takahiro Nakajima, Division of Thoracic Diseases, Chiba Cancer Center, 666-2 Nitona-cho, Chuo-ku 260-8717, Chiba, Japan. Phone: 81-43-264-5431; Fax: 81-43-262-8680; E-mail: nakajii@fc.med.miyazaki-u.ac.jp.

doi: 10.1158/1078-0432.CCR-10-0099

Translational Relevance

Acquisition of proper tissue samples for molecular analysis is not always an easy task; however, information obtained from such specimens is essential for the selection of appropriately targeted cancer therapies. This study shows that endobronchial ultrasound-guided transbronchial needle aspiration (EBUS-TBNA) contributes to the resolution of this issue in lung cancer because tissue samples obtained by EBUS-TBNA can be successfully used to assess the presence of echinoderm microtubule–associated protein-like 4–anaplastic lymphoma kinase fusion genes. We have shown that EBUS-TBNA samples could be subjected to immunohistochemistry, fluorescent *in situ* hybridization, and reverse transcription-PCR analysis. EBUS-TBNA for the assessment of mediastinal and hilar adenopathy is a practical tool that can be used in the molecularly targeted treatment era for lung cancer.

patients with lung cancer (5, 6). EBUS-TBNA is generally accepted to be as safe as standard bronchoscopy, less invasive than mediastinoscopy, and of high diagnostic quality. Compared with conventional fine-needle aspiration, EBUS-TBNA is an outstanding procedure with respect to its extremely low morbidity and its repeatability; fine-needle aspiration could cause pneumothorax, and repeated sampling might be difficult to perform.

In this study, we analyzed the feasibility of EBUS-TBNA for the detection of *EML4-ALK* fusion genes. We also retrospectively analyzed the clinicopathologic characteristics of *ALK*-positive lung cancer cases with mediastinal and/or hilar lymph node metastasis.

Materials and Methods

Patients

From April 2008 to July 2009, 112 cases with proven hilar and/or mediastinal lymph node metastasis of NSCLC were enrolled; re-sliced specimens for histologic examination were available for 109 of these cases. Independent pathologists (D. Ikebe and M. Itami) reviewed all cases and histologically confirmed the presence of cancer cells in each specimen. Morphologic features detected with H&E staining were also recorded, and mucin production was evaluated by Alcian blue staining. First, samples were screened for *ALK* abnormalities using immunohistochemistry. Cases that were determined to be *ALK*-positive or suspicious by immunohistochemistry in our laboratory were subjected to additional evaluation by FISH and immunohistochemistry restaining by an independent pathologist (K. Takeuchi) at the Division of Pathology, The Cancer Institute, Japanese Foundation for Cancer Research. Final confirmation was performed by direct sequencing of *EML4-ALK* fusion cDNAs using EBUS-TBNA histologic cores that had been preserved at −80°C. *EGFR* gene mutation status was also evaluated in all EBUS-TBNA samples. Associations between the presence of *ALK* fusion genes and clinicopathologic characteristics were retrospectively analyzed from medical records.

EBUS-TBNA

In all cases, chest computed tomography was performed prior to EBUS-TBNA. Brain magnetic resonance imaging, enhanced computed tomography, and bone scintigraphy were also performed for clinical staging of each case. EBUS-TBNA was performed for lymph nodes >5 mm in short axis on chest computed tomography. To obtain a histologic core, a dedicated 22-gauge needle equipped with an internal stylet was used. After the initial puncture, the internal stylet was used to clean out the internal lumen that was clogged with bronchial tissue (Fig. 1A). The internal stylet was removed, and negative pressure was applied using a syringe. The needle was then moved back and forth inside the lymph node. Finally, the needle was retrieved, and the internal stylet was used to push out the histologic core (6). Each histologic core was divided into two samples: one was fixed with formalin and used for histologic diagnosis, and the other was mixed with Allprotect Tissue Reagent (Qiagen) following the instructions of the manufacturer, and stored at −80°C.

ALK detection with immunohistochemistry

For detection of the *ALK* fusion gene, we applied the iAEP method, which incorporates an intercalating antibody between the primary antibody to *ALK* and dextran polymer–based detection reagents (4).

Histologic cores obtained by EBUS-TBNA were routinely fixed in 20% neutralized formalin and embedded in paraffin. Blocks were sliced at a thickness of 4 μm, and sections were placed on silane-coated slides. Antibody preparations specific for the intracellular region of *ALK* (5A4, Abcam) were subjected to immunohistochemical staining according to standard protocols using dextran polymer reagents (anti-mouse immunoglobulin, EnVision+DAB System; Dako). The *ALK* antibody (5A4) was used at a dilution of 1:50. For antigen retrieval and deparaffinization, slides were heated for 20 minutes at 98°C in Target Retrieval Solution (low pH; Dako) with PT-link (Dako). Pretreated slides were positioned in a programmable AutoStainer instrument (EnVision System; Dako). Following the immunohistochemical program, slides were incubated at room temperature first with Peroxidase Blocking Solution (Dako) for 5 minutes and then with *ALK* antibody (5A4, 1:50; Abcam) for 30 minutes. Following application of the iAEP method, which has been described in detail elsewhere (4), we included an incubation step of 15 minutes at room temperature with intercalated immunoglobulin (Mouse-LINKER; Dako) to increase the detection sensitivity. Immune complexes were then detected using the dextran polymer reagent for 30 minutes. 5A4-positive cells were stained with 3,3′-diaminobenzidine for 5 minutes, and nuclei were then stained with hematoxylin for 2 minutes.

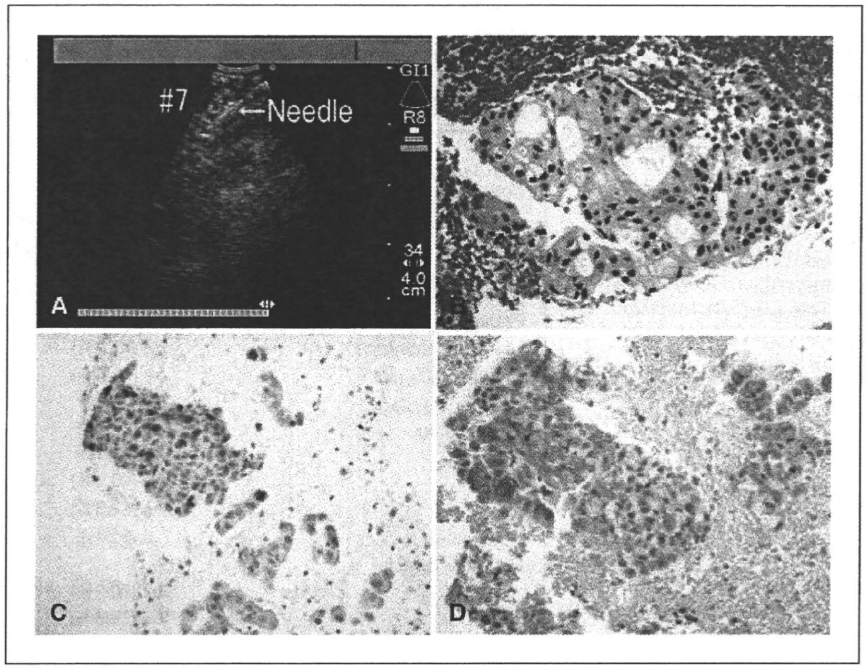

Fig. 1. Diagnosis of metastatic nodes by EBUS-TBNA. A, lymph node sampling by EBUS-TBNA. B, adenocarcinoma was revealed in the EBUS-TBNA sample. C, mucin production was observed by Alcian blue staining. D, immunohistochemistry with an anti-*ALK* antibody showed *ALK* fusion protein positivity in lung adenocarcinoma cells.

The samples obtained with EBUS-TBNA were small, paraffin-embedded biopsy specimens, which might limit the utility of immunohistochemistry. To avoid false-negative diagnosis, the first immunohistochemical procedure was used as a screening test to define three categories with which to judge the first run. Cancer cells were defined as "positive" if staining was as strongly positive as a positive control (clinical lung cancer tissues previously defined as positive by both molecular and immunohistochemistry analyses) and a fine, granular cytoplasmic staining pattern was observed. Cancer cells that showed no staining were classified as "negative." The "suspicious" classification was defined as the presence of weakly stained cells that were considered difficult to differentiate from background staining. While using these categories, we further subdivided the suspicious category into "probably positive" and "probably negative" categories. Probably positive meant that the tumor cells stained, but not strongly, whereas probably negative indicated very weak staining that was difficult to differentiate from background staining. After the screening immunohistochemistry, suspicious cases were re-tested by immunohistochemistry in addition to FISH by a second independent pathologist (K. Takeuchi).

Fluorescence *in situ* hybridization

To further confirm the *ALK* genomic rearrangement, two FISH assays were performed: an *ALK* split assay and an *EML4-ALK* fusion assay. Unstained sections were processed with a Histology FISH Accessory Kit (Dako), subjected to hybridization with fluorescently-labeled bacterial artificial chromosome clone probes for *EML4* and *ALK* (self-produced probes; *EML4* RP11-996L7, *ALK* RP11-984I21, and RP11-62B19) or for genomic regions upstream and downstream of the *ALK* breakpoint (Dako), stained with 4,6-diamidino-2-phenylindole, and examined with a fluorescence microscope (BX51; Olympus; ref. 7). FISH analysis was performed at the Division of Pathology, The Cancer Institute, Japanese Foundation for Cancer Research (K. Takeuchi). The FISH positivity criteria for EBUS-TBNA samples were defined as "over 50% cancer cells." As EBUS-TBNA samples are small biopsy samples, entire tumor cells in the paraffin-embedded section were evaluated.

RT-PCR and direct sequencing

Frozen histologic cores obtained by EBUS-TBNA were used to extract RNA. All immunohistochemistry-positive or suspicious cases were subjected to direct sequencing of the fusion cDNAs. RNA was extracted from frozen samples using the AllPrep DNA/RNA mini kit (Qiagen), and cDNA cloning was performed with the High Capacity RNA-to-cDNA Kit (Applied Biosystems). For RT-PCR analysis of *EML4-ALK*, we used primer sequences that have been described previously (2). After PCR amplification, PCR products were analyzed using agarose gel electrophoresis. RT-PCR products were extracted from gel slices using the QIAquick Gel Extraction Kit (Qiagen). Purified products were then sequenced with a capillary sequencer. Resultant nucleotide sequences were compared with previously reported sequences for determination of the *EML4-ALK* variant. *EGFR* mutation status was also examined using the peptide nucleic acid/locked nucleic acid PCR clamp method for samples obtained with EBUS-TBNA (8).